remote sensing

MDPI

Article

Modeling Potential Habitats of Macrophytes in Small Lakes: A GIS and Remote Sensing-Based Approach

Bastian Robran [1,*], Frederike Kroth [1], Katja Kuhwald [1], Thomas Schneider [2] and Natascha Oppelt [1]

[1] Earth Observation and Modelling, Department of Geography, Kiel University, Ludewig-Meyn-Str. 8, 24098 Kiel, Germany
[2] Aquatic Systems Biology Unit, Limnological Research Station Iffeldorf, Department of Ecology and Ecosystem Management, Technical University of Munich, Hofmark 1-3, 82393 Iffeldorf, Germany
* Correspondence: robran@geographie.uni-kiel.de

Abstract: Macrophytes, which are foundational to freshwater ecosystems, face significant threats due to habitat degradation globally. Habitat suitability models are vital tools used to investigate the relationship between macrophytes and their environment. This study addresses a critical gap by developing a Geographic information system-based HSM tailored for small lakes, which are often overlooked in ecological studies. We included various abiotic predictors to model the potential macrophyte habitat for several small lakes in southern Bavaria (Germany). Key factors such as the distance to groundwater inflow, depth, availability of photosynthetically active radiation (PAR), and littoral slope were identified as significant predictors of macrophyte occurrence. Notably, the HSM integrates remote sensing-based data to derive PAR availability at the growing depths of the macrophytes using Sentinel-2 MSI data. Integration of an MSI-based time series of PAR availability enabled the introduction of a temporal component allowing monitoring and predicting changes in macrophyte habitats over time. The modeled habitat suitability score correlates highly (R = 0.908) with macrophyte occurrence. We see great promise in using habitat modeling for macrophytes as a tool for water management; in particular, the use of Sentinel-2 MSI data for habitat suitability modeling holds promise for advancing water management. By demonstrating the efficacy of GIS- and remote sensing-based HSM, we pave the way for future applications of this innovative approach in ecological conservation and resource management.

Keywords: habitat suitability; macrophytes; inland waters; remote sensing; GIS; habitats; lakes

Citation: Robran, B.; Kroth, F.; Kuhwald, K.; Schneider, T.; Oppelt, N. Modeling Potential Habitats of Macrophytes in Small Lakes: A GIS and Remote Sensing-Based Approach. *Remote Sens.* **2024**, *16*, 2339. https://doi.org/10.3390/rs16132339

Academic Editors: Michael Nones, Paolo Paron and Maria Nicolina Papa

Received: 30 April 2024
Revised: 21 June 2024
Accepted: 22 June 2024
Published: 26 June 2024

1. Introduction

Freshwater ecosystems are among the most endangered habitats worldwide [1,2]. They are valuable for studying aquatic ecosystems under changing conditions. Lakes, as relatively closed ecosystems with distinct cycles, food webs, and species pools, serve as scaled-down model systems for global change studies [3,4].

Macrophytes function as foundational species [5] in lakes around the world. They are photosynthetic aquatic organisms, visible to the naked eye, including charophytes, bryophytes, pteridophytes, and spermatophytes [6]. Macrophytes play key roles in nutrient cycling [7,8], structuring phytoplankton [9], zooplankton communities [10,11], and modifying habitats [12,13]. They enhance habitat complexity [14] and influence trophic webs by providing detritus [15,16]. Additionally, they provide ecosystem services such as water purification, disease management, wastewater treatment, erosion regulation, and food provision [17]. At the same time, however, various anthropogenic threats and climatic shifts cause a decline in macrophyte diversity globally [18,19]. As photosynthetic organisms, macrophytes rely on light within the range of photosynthetically active radiation (PAR) [20]. In aquatic ecosystems, PAR decreases with depth, quantified by the attenuation coefficient (KdPAR), which is influenced by turbidity [20]. Climate change is expected to increase turbidity [21], thereby raising KdPAR and reducing PAR, adversely affecting macrophytes.

In Europe, authorities map macrophytes in lakes larger than 50 ha within a three-year cycle, leaving a significant research gap for smaller lakes, which constitute 80 to 90% of European lakes [22]. However, high monitoring costs and time constraints make comprehensive macrophyte monitoring challenging. Thus, decision-makers require cost-effective approaches to support macrophyte monitoring in small lakes. To address this, we aim to use models that predict macrophyte distribution and potential habitats, which can be used to support monitoring and identify areas of interest that are not included in regular monitoring.

Modeling techniques are widely used for studying species–environment relationships [23]. These techniques facilitate the mapping of current and potential species distributions and predict how these distributions may change in response to environmental alterations. Such models can provide valuable insights into environmental management decisions [24]. However, the accuracy of model predictions depends heavily on the quality and quantity of input parameters, and their transferability is often limited [25–27]. Model development requires careful selection of predictors, models, and validation methods tailored to the species, region, and spatial and temporal scale of interest [23,28]. In this study, we use the term 'habitat suitability model' (HSM) to describe potential habitats of freshwater macrophytes [29]. In the literature, however, several different terms are used interchangeably, e.g., habitat suitability model, species distribution model, or ecological niche model [30,31].

In general, a combination of various scale-dependent abiotic and biotic factors influence the distribution and abundance of macrophytes in lakes [32–34]. Abiotic factors comprise local or lake-specific environmental factors, such as water chemistry [35], temperature [36], littoral slope [37,38], and the availability of PAR [39,40]. They are more influential than broader geographic, climatic, or historical conditions [41,42]. Biotic factors influencing macrophyte habitats constitute herbivory, epiphytic growth, and competition among plants [15,43–45]. However, in our study region, there is limited understanding of such biotic interactions and their role in determining macrophyte diversity. We, therefore, focus on abiotic factors and their potential to characterize the potential macrophyte habitat, laying the foundation for a model-based analysis of macrophyte occurrence in our study region. To this end, we developed an HSM using geographic information system (GIS) techniques and remote sensing data for a series of small freshwater lakes in southern Germany. Our focus is on abiotic factors affecting submerged and floating-leaved angiosperms and charophytes, referred to as 'macrophytes'. Concerning the integration of remote sensing data, we focus on inferring the availability of PAR on the lake bottom. PAR availability, traditionally determined using proxies such as measurements of Secchi disk depth, has been identified as an important predictor of macrophyte occurrence that can be inferred from remote sensing data with high temporal and spatial resolution [46]. Despite its potential, to the best of our knowledge, remote sensing-derived PAR availability has not been incorporated into HSMs or other aquatic ecological models.

Therefore, our objectives are to (1) determine the potential habitat of macrophytes in small lake systems, (2) discuss the HSM as a practical tool for decision-makers and water resource managers, and (3) illustrate the added value of remote sensing for modeling and monitoring in small-scale freshwater environments.

2. Materials and Methods

2.1. Study Site

The Osterseen Lake District (47.79°N, 11.30°E) is located in southern Bavaria (Germany) and developed from dead-ice formations during the last glacial period. The pre-alpine region experiences a temperate climate with high annual precipitation, averaging 1250.4 mm [47], and moderate annual temperatures, with a mean of 8.6 °C [48].

There are 19 interconnected lakes in the Lake District with a total surface area of 215 hectares and maximum depths ranging from 5 to 30 m. Despite the area's high precipitation, most lakes are sustained either directly or indirectly through other lakes by groundwater inflow (Figure 1). They are notably categorized as hard-water lakes due to their elevated $CaCO_3$ concentrations, resulting in a saturation index (Ω) of 4.8 ± 1.2 [49] and slight alkalinity (pH ranging from 7.5 to 8.8) [50]. Experts assumed that initially, all the lakes were oligotrophic [51]. However, ongoing agricultural activities around the southernmost lakes and municipal wastewater inflows from the village of Iffeldorf until the mid-1980s led to eutrophication [50]. Nowadays, the lakes display a distinct trophic gradient, with the southern lakes exhibiting eutrophic conditions and the northern lakes maintaining oligotrophic conditions (see Figure 1; Table 1) [52]. Based on this gradient, the lakes are categorized as southern (eutrophic), northern (oligotrophic), and central and eastern (meso- and meso-oligotrophic) lakes, presenting a unique model system to address ecological questions.

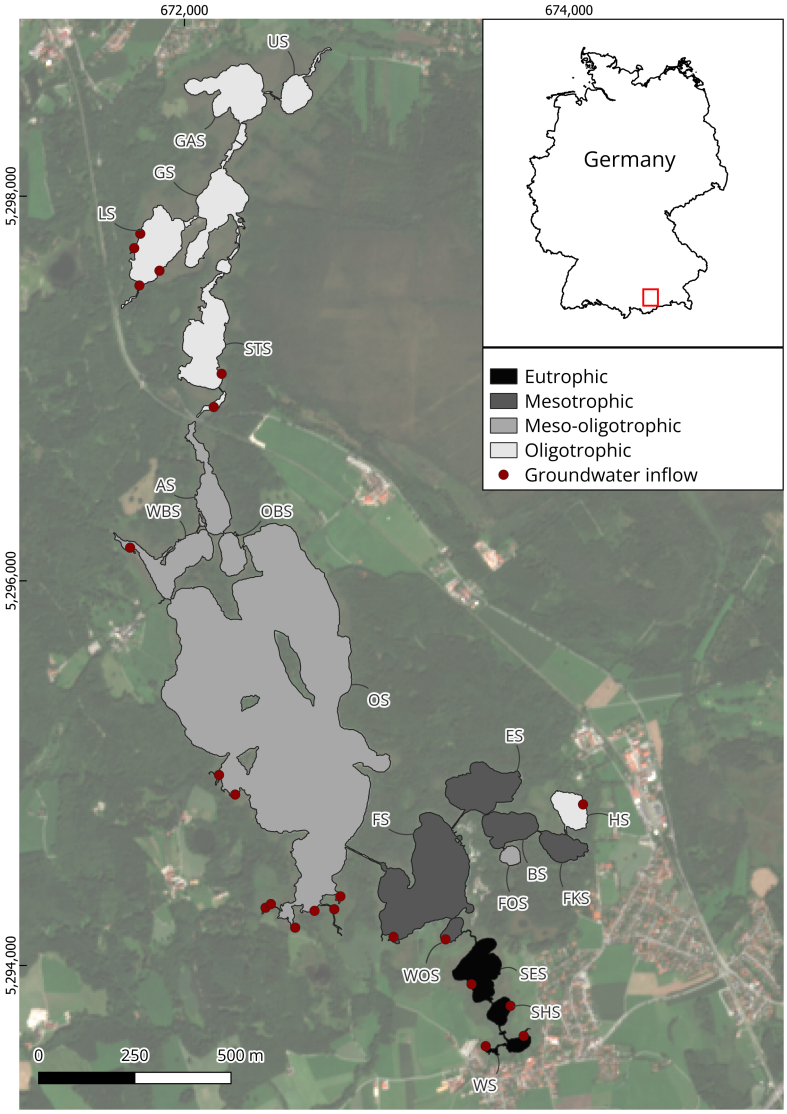

Figure 1. The Osterseen Lake District in Upper Bavaria, Germany. The trophic state of the lakes (white to black) and groundwater inflow locations (red dots). Basemap: Sentinel-2A MSI L2A 11.08.2023 T32, CRS: WGS 84 EPSG:32632.

Table 1. List of lakes and abbreviations in the Osterseen Lake District.

Lake Name	Abbr.	Trophic State	Surface Area [ha]	Max. Depth [m]	Cluster
Ursee	US	Oligotrophic	2.75	11.8	northern
Gartensee	GAS	Oligotrophic	7.89	14.2	
Gröbensee	GS	Oligotrophic	7.81	15.8	
Lustsee	LS	Oligotrophic	7.16	18	
Stechsee	STS	Oligotrophic	9.50	15.4	
Ameisensee	AS	Meso-oligotrophic	5.28	19.8	central
Öst. Breitenauersee	OBS	Meso-oligotrophic	2.40	16.3	
West. Breitenauersee	WBS	Meso-oligotrophic	6.49	17.8	
Ostersee	OS	Meso-oligotrophic	118.48	30.1	
Eishausseee	ES	Mesotrophic	6.99	19.8	eastern
Herrensee	HS	Oligotrophic	2.72	11.5	
Bräuhaussee	BS	Mesotrophic	3.96	13.1	
Fischkaltersee	FKS	Mesotrophic	2.71	11.9	
Forchensee	FOS	Meso-oligotrophic	0.84	9.4	
Fohnsee	FS	Mesotrophic	19.65	24.1	southern
Wolfelsee	WOS	Mesotrophic	1.02	6.1	
Sengsee	SES	Eutrophic	5.03	15.1	
Schiffhüttensee	SHS	Eutrophic	1.35	6.4	
Waschsee	WS	Eutrophic	1.08	5.5	

Due to the temperate climate, the lakes are dimictic, i.e., they experience two periods of full water column mixing in the spring and fall. However, Lake ES is an exception, as it is only partially mixed and, thus, classified as meromictic [50]. During the stratified phases of the lakes, some of the southern lakes are also subject to cycles of calcite supersaturation [49]. During these states, the affected lake waters are highly turbid with Secchi depths < 2 m due to calcite precipitation within the water column. Additionally, high calcite conditions favor phytoflagellate (*Phacotus lenticularis*) abundances, which may further influence the carbonate chemistry within the lakes [49]. The northern lakes, except Lake LS, experience surface inflows from the adjacent Staltacher Moor, which introduce high levels of humic acid into the lake water and lead to a brownish water color.

2.2. Modeling Habitat Suitability

Habitat suitability refers to a habitat's capacity to sustain specific species [29]. It is linked to environmental factors, influencing the likelihood of the species' presence in a particular area [53]. As previously mentioned, human activities are major contributors to the decline in lake habitats [18]. Therefore, studying lake habitat suitability is crucial as it provides insights into their quality.

We used a linear additive approach to forecast the suitability of the lakes in our study region for macrophyte occurrence. Therefore, the HSM determines the environmental abiotic factors that specific macrophytes prefer or avoid to assess the presence of these factors across a landscape, resulting in a suitability index. Using a geographic information system (GIS), these index values can be visualized and studied to identify suitable habitat areas for the species. It is essential to understand that the modeling results reflect the potential suitability of a habitat for a species, not its actual presence. Model inputs were selected based on the literature [37,38,54–56], comparable studies [57], and region-specific observations; these inputs encompass bathymetric data, littoral slope, PAR availability, and the distance to groundwater inflows.

The HSM was constructed using the most important abiotic predictors to generate an overall suitability score for each pixel. We employed the method described by Fleming et al. [57], which was adopted from work by Malczewski [58]. Using this method, non-binary layers (x_i) were combined into a dimensionless score, where equal weighting of

each input simplifies to the mean value of the layers ($\overline{x_i}$). Binary layers for PAR availability ($PAR_{1/0}$) served to pre-select viable habitats as follows:

$$HSS = PAR_{1/0} * \overline{x_i} \quad (1)$$

The output of the model is a dimensionless habitat suitability score (HSS), set to the range from 0 to 100, which expresses the habitat suitability for freshwater macrophytes during the growth season from March to September.

2.3. Model Input

In this section, we outline the input parameters for our HSM and describe how we derived the inputs from raw data.

2.3.1. Satellite Data

We used Sentinel-2 MSI data to gather spatiotemporal information about direct irradiance, irradiance geometry, and K_dPAR (see Figure 2). The sensor was selected due to its high data availability, good radiometric resolution, sufficient spatial resolution, and high temporal resolution. A total of 139 level-1 top-of-atmosphere scenes (processing baseline 05.09) were acquired from January to December 2023 with a maximum cloud coverage threshold of 75% from the Copernicus Data Space Environment. These scenes underwent atmospheric correction using the ACOLITE processor (update from 26 February 2024) following the dark spectrum fitting approach using the SWIR-based glint correction algorithm [59,60]. To mitigate the effects of land adjacency and filter out atmospheric conditions with unreasonably high NIR values retrieved by ACOLITE, the land–water masking wavelength was adjusted from the default 1600 nm to the 865 nm bands, and the SWIR/NIR masking threshold increased to 0.05.

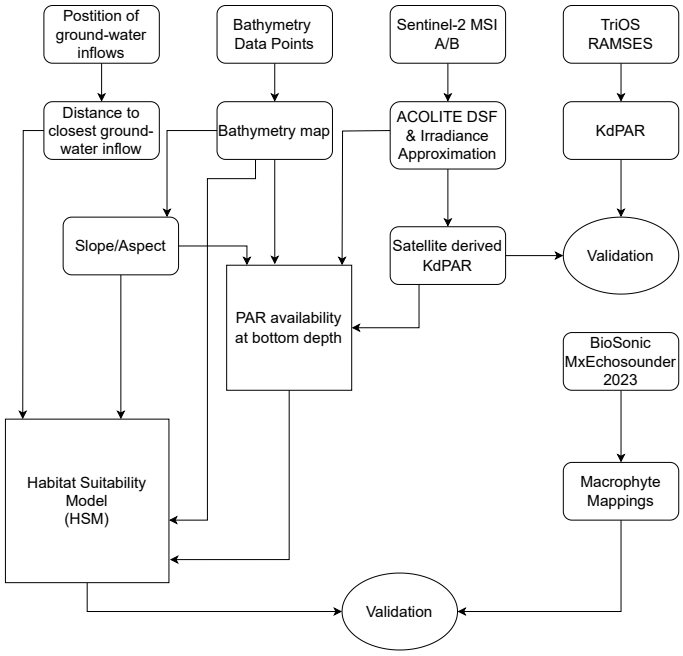

Figure 2. Overview of the workflow including data processing (round-cornered boxes), HSM and PAR model construction (square boxes), and validation (oval boxes).

ACOLITE provides an implementation of the quasi-analytical algorithm (QAAv6) to estimate inherent optical water properties [61]. Two algorithms are available for K_dPAR retrieval using QAAv6, i.e., the "QAAv6-KPAR-Lee" [62] and the unpublished second version fit to Kd_{490} QAAv6 outputs named "QAAv6-KdPAR-Nechad". For this study, both methods were evaluated. To do so, we first applied ACOLITE's inherent water masking and

the normalized difference water index (NDWI) to select valid water pixels. Then we used the normalized ratio between the 492 nm and 665 nm MSI bands to mask shallow water pixels. The remaining water pixels were then aggregated to determine the average K_dPAR, which is used as an input parameter to the HSM for each lake. For validation, a square of 3 × 3 10 m MSI pixels was extracted at the geolocation of in situ K_dPAR measurements. The median of the 9 pixels was combined into a macro-pixel. We made spatiotemporal match-ups for the same day (±12 h) and geolocation (±20 m) of the in situ measurements, which are described further in the next section.

Figure 3 shows a comparison of satellite-derived K_dPAR and in situ-measured K_dPAR using the TriOS RAMSES radiometer. Table 2 provides additional statistics and accuracy measures. A total of 21 spatiotemporal match-ups between in situ and remotely sensed data were obtained. Figure 3 and Table 2 show that the two algorithms performed similarly. The in situ measurements ranged from 0.47 to 1.05 m^{-1}. In comparison, the remotely sensed data covered a broader range, as follows: 0.37 to 1.22 m^{-1} using the Nechad algorithm and 0.41 to 1.39 m^{-1} using the Lee algorithm. The satellite-derived K_dPAR tended to underestimate lower values (<0.8 m^{-1}) and overestimate higher ranges, resulting in a mean bias error of 0.05 m^{-1} for K_dPAR_{Nechad} and 0.04 m^{-1} for K_dPAR_{Nechad} (Table 2). Specifically, K_dPAR_{Lee} underestimates to a lesser extent than K_dPAR_{Nechad} for lower values. For higher K_dPAR values, however, our analysis indicates that K_dPAR_{Lee} overestimates more than K_dPAR_{Nechad}. The intercept and slope of the linear regression fit shown in Table 2 and Figure 3 suggest that K_dPAR_{Nechad} was more accurate across the entire range of K_dPAR. Nevertheless, most of our data were in the lower range of <0.8 with a mean in situ K_dPAR of 0.63. Therefore, the Pearson correlation coefficient r and the coefficient of determination R^2 favor K_dPAR_{Lee}, as they underestimate less at lower values. Consequently, we selected K_dPAR_{Lee} for further processing.

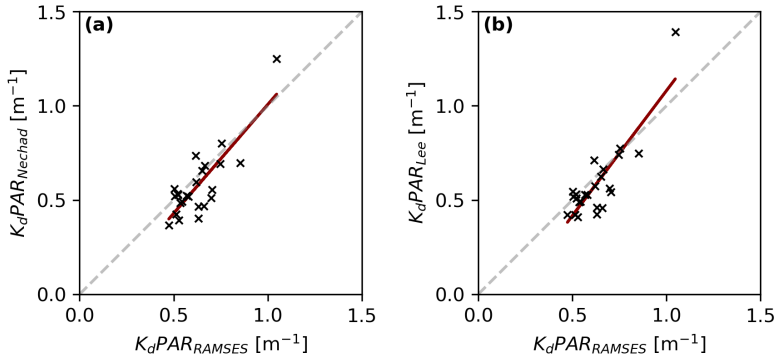

Figure 3. Macropixel (30 × 30 m) match-ups from Sentinel-2 MSI and in situ K_dPAR measurements using the QAAv6 Nechad algorithm (**a**) and the QAAv6 Lee algorithm (**b**).

Table 2. Statistical overview on in situ and remotely sensed K_dPAR and match-up quality metrics (MBE is the mean bias error). All values refer to m^{-1} except for R and R^2.

	Mean	Min	Max	Slope	Intercept	r	R^2	MBE
$KdPAR_{RAMSES}$	0.63	0.47	1.05					
$KdPAR_{Nechad}$	0.58	0.37	1.25	1.22	−0.19	0.85	0.73	0.05
$KdPAR_{Lee}$	0.59	0.41	1.39	1.4	−0.29	0.88	0.77	0.04

The algorithm by Lee et al. [61] was applied to the entire dataset to compute K_dPAR. Figure 4 displays the results for each lake as mean values per month. Data were available for every month in 2023 except for March. During this month, cloud coverage and atmospheric conditions prevented retrieving K_dPAR from Sentinel-2 MSI data. Figure 4 illustrates temporal patterns, with clear water phases in May and November (low K_dPAR) and phases

of high attenuation from August to October in almost all lakes. Differences between lakes within the same months were less pronounced.

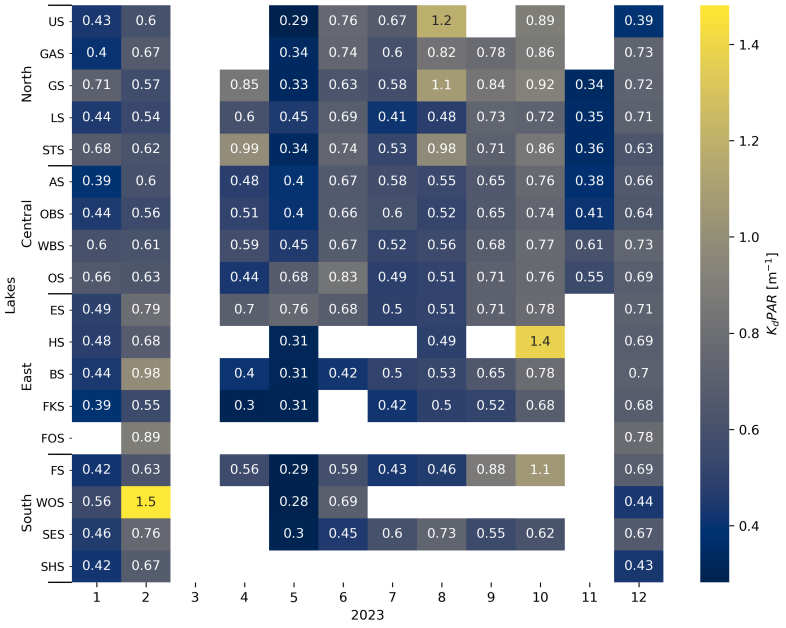

Figure 4. Monthly means of K_dPAR for each lake in 2023 derived from Sentinel-2 MSI data using the QAAv6 Lee algorithm; the months (1 = January and 12 = December) are shown on the X-axis.

Finally, we also approximated the clear sky downwelling direct solar irradiance ($E_d(\lambda)$) for a horizontal surface from Sentinel-2 using ACOLITE's irradiance function (https://github.com/acolite/acolite/issues/61, accessed on 26 Febuary 2024). For each Sentinel-2 MSI scene, a single $E_d(\lambda)$ value was retrieved along with the solar zenith and azimuth angles.

2.3.2. Radiometric Field Data

We used in situ data measured during the summer of 2023 to validate the remote sensing K_dPAR results (see Figure 2). Spectral measurements of irradiance and radiance with the TriOS RAMSES radiometer from above the water surface to a depth of 5 m were used to calculate K_dPAR.

$K_d(\lambda)$ was calculated as follows:

$$K_d(\lambda) = \frac{1}{z} * log(\frac{E_d0(\lambda)}{E_dz(\lambda)}) \quad (2)$$

ref. [63], where z denotes the water depth, $E_d0(\lambda)$ denotes the downwelling irradiance per wavelength, λ denotes the below water surface, and $E_dz(\lambda)$ denotes downwelling irradiance per wavelength at water depth z.

$K_d(\lambda)$ was then transformed to average K_d within the range of PAR, hereafter referred to as K_dPAR:

$$K_dPAR = \frac{\int_{400_{nm}}^{700_{nm}} K_d(\lambda)}{700 - 400} \quad (3)$$

2.3.3. Bathymetric Data

Lake bathymetry or water depth has been extensively studied in relation to macrophyte occurrence and growth [38,54,56,64]. Previous studies have mainly focused on maximum depths determined by PAR availability or under-water pressure. However, little is known about minimum depths, which may also play an important role in habitat suitability in our study region. In our HSM, water depth was treated as a positive indicator,

with greater depth considered more suitable, as the maximum depth is constrained by a threshold for minimum PAR availability (see the subchapter on PAR availability). We used water depth data collected by the Bavarian State Office for the Environment in 2001 along transects across the whole lake chain using a sonar device [65]. The bathymetry data (n = 141,046) were interpolated individually for each lake using ordinary kriging (R Version 4.2.2. [66], R package: gstat [67,68]), to a cell size of 2 × 2 m. The resulting gridded bathymetry is shown in Figure 5. To use water depth as a predictor for the HSM, the depth was standardized to a range between 0 and 1 using the method presented by Fleming et al. [57]:

$$V_z = 1 - \frac{z_i - z_{min}}{z_{max} - z_{min}} \quad (4)$$

where z_i is the original depth value at a particular pixel, z_{min}, and z_{max} are the minimum and maximum depth values of the dataset, and V_i is the standardized depth value for that particular pixel.

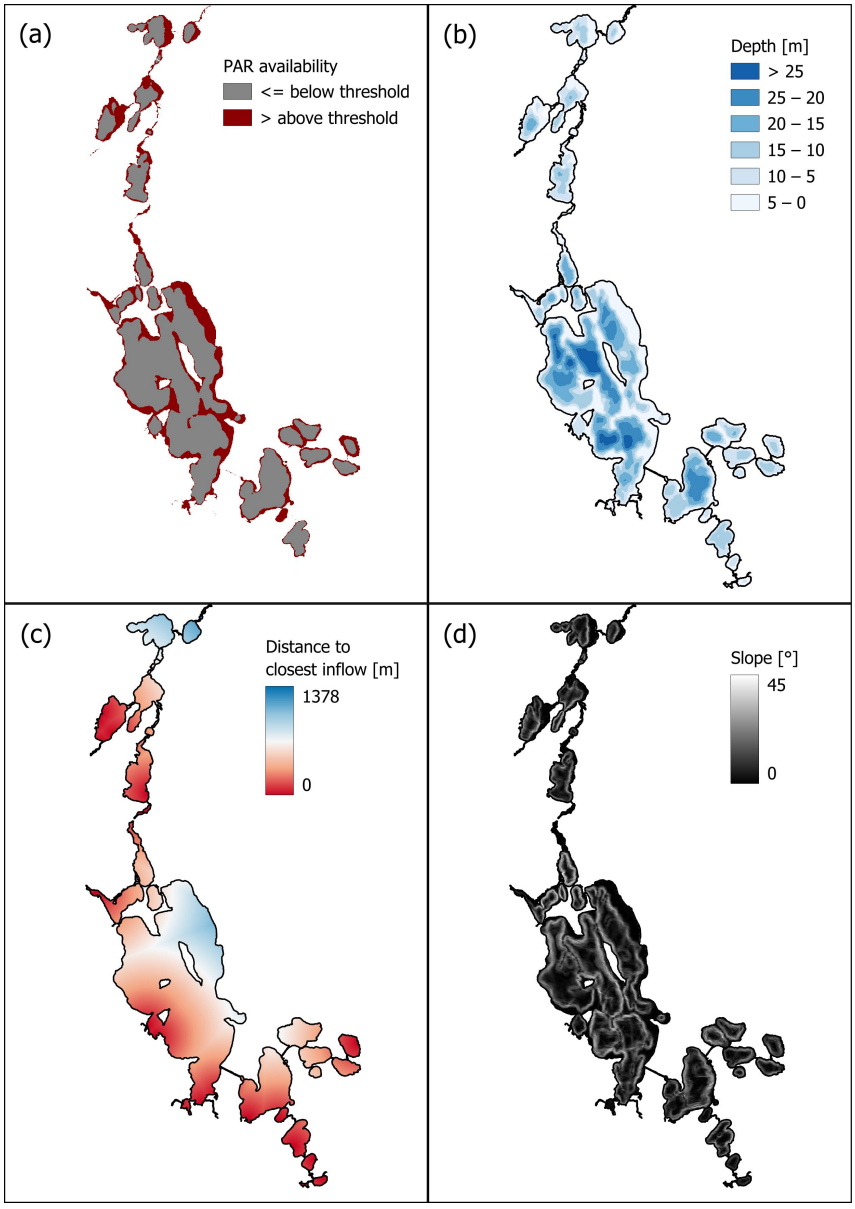

Figure 5. Abiotic predictors for the HSM: (**a**) PAR availability above threshold, (**b**) water depth, (**c**) distance to the nearest groundwater inflow, and (**d**) littoral slope.

2.3.4. Littoral Slope

Similar research has already used the littoral slope as a predictor of suitable macrophyte habitats [57]. This approach is based on the findings of Duarte and Kalff [37], who identified the littoral slope as a key predictor of macrophyte biomass. Moreover, Florêncio et al. [69] also established a significant correlation between macrophyte abundance and littoral slope. They suggest that gentle-sloping habitats are more suitable than steep-sloping habitats. We calculated the littoral slope and the aspect from our bathymetric data (see Figure 2) using the Python package xarray-spatial (version 0.3.5, https://github.com/makepath/xarray-spatial, accessed on 10 August 2022). Both littoral slope (see Figure 5d) and aspect were used as inputs to calculate PAR availability. As a predictor of the HSM, the littoral slope was standardized from degrees to a range between 0 and 1 following Fleming et al. [57] as in Equation (4).

2.3.5. PAR Availability

The availability of PAR has long been recognized as a key limiting factor for macrophyte occurrence [39,40,56,70,71]. Therefore, we assume that PAR availability is an important indicator for identifying potential macrophyte habitats in our study region. We define PAR according to Mõttus et al. [72] as being the electromagnetic radiation in the wavelength region between 400 and 700 nm. PAR availability was estimated throughout the water column and at bottom depth considering water-depth/bathymetry, downwelling direct irradiance, irradiance geometry, irradiance exposition, attenuation of PAR within the water column, and surface reflectance/albedo. For $E_d(\lambda)$ and irradiance geometry, we used the data extracted with ACOLITE (see Figure 2). $E_d(\lambda)$ in [mW m^{-2} nm^{-1}]. Processing to PAR in [µ mol m^{-2} s^{-1}] was conducted using the equation adopted from Mõttus et al. [72]:

$$PAR = \frac{1}{hc} \frac{\int_{400_{nm}}^{700_{nm}} E_d(\lambda)\lambda d\lambda}{\int_{400_{nm}}^{700_{nm}} E_d(\lambda) d\lambda} \quad (5)$$

with h being Planck's constant in [µJ/s] and c the speed of light in [m/s]. The availability of PAR at the surface (PAR_s) was then calculated using the sun's zenith angle (θ) to account for Lambert's cosine law:

$$PAR_s = PAR * cos(\theta) \quad (6)$$

For PAR availability at the lake bottom, we had to consider the effect of refraction as described by Snell's law and consider the exposure toward the sun, i.e., littoral slope and aspect. Thus, the angle of incidence of PAR at the bottom depth was calculated using Equation (7):

$$\theta_Z = \cos(\arccos(\theta) \cdot \cos(\theta_{tilt}) + \sin(\theta) \cdot \sin(\theta_{tilt}) \cdot \cos(\alpha - \alpha_{aspect})) \quad (7)$$

where θ_{tilt} is the tilt of the lake bottom, α_{aspect} refers to the aspect of the lake bottom, α is the sun azimuth angle and θ the sun zenith angle adjusted for refraction. All angles were converted to radians beforehand. The resulting θ_z represents the angle of incidence for PAR at the lake bottom, also in radians. This angle was needed for the last step, where we calculated PAR availability at the lake bottom (PAR_z) using the Lambert–Beer law. This law describes the decrease in PAR throughout the column of water [73], expanding it to include irradiance geometry, as described in Equation (8).

$$PAR_Z = PAR * (1 - 0.03) * e^{-K_{dPAR} * \frac{z}{sin(\theta_p)}} * \theta_z \quad (8)$$

where z is the water depth and θ_p is the refraction-adjusted solar zenith angle, accounting for angle-specific path lengths through the water column. Based on our radiometric in situ measurements, an average albedo of 3% for the water surface was assumed. Effects of

mirror-like reflection, such as sun-glint, were not considered in estimating PAR availability at the lake bottom.

To incorporate PAR availability into the model, the data were aggregated along the temporal axis. Consequently, we calculated the median PAR availability for each pixel for the growing season (March to September 2023). Unlike the other predictors, PAR availability was implemented in the model as binary input, represented by values of 1 or 0. A minimum threshold of PAR availability must be exceeded during the growing season to consider a pixel as a potentially suitable habitat (value = 1). We selected a minimum threshold of 1.3% for PAR availability based on the analysis of hydroacoustic macrophyte mappings (see subchapter "Model Validation") and our calculations of PAR availability. This threshold will be discussed in the Discussion section. The resulting spatial distribution of PAR availability in binary format is displayed in Figure 5a.

2.3.6. Distance to Groundwater Inflow

Some lakes in the Osterseen Lake District are fed directly by groundwater sources while others are not [50]. As we expect the influence of direct cold groundwater inflow to be an important parameter for the presence or absence of macrophytes, an analysis of its effect seems promising. The groundwater sources provide cold inflow (around 8–10 °C) throughout the year, moderating the warm temperatures during summer and the lower temperatures in winter [50]. Furthermore, groundwater inflow has been associated with higher conductivity and lower pH levels in the respective lakes [50]. Therefore, it was assumed that groundwater inflow could serve as a plausible predictor for the spatial distribution of macrophytes and consequently included in our HSM.

To achieve this, we digitized geospatial data on the locations of groundwater inflows from Zwirglmaier et al. [50] in QGIS. Then, the Euclidean distance to the nearest groundwater inflow for each pixel was calculated with the *spatial.distance.euclidean* function of the *SciPy* Python package (version 1.10.1, https://scipy.org/, accessed on 27 November 2023), which resulted in the data shown in Figure 5c. The obtained parameter was considered a negative predictor, where a greater distance from an inflow corresponds to a less suitable habitat. It was also standardized to values between 0 and 1 following the procedure of Fleming et al. [57].

2.4. Model Validation

Since the HSM presented in this study is built to identify potential habitat suitability rather than actual habitats, validation is only partially viable. However, evaluating how well actual habitats coincide with modeled potential habitat suitability should provide a sufficient basis to discuss the validity of our model. We, therefore, conducted hydroacoustic field mappings of actual macrophyte habitats in July and August 2023 using the BioSonics Habitat Echosounder MX-200 and processed the data with the corresponding software Visual Aquatic Version 1.0.0.13146 (BioSonics Inc. Seattle, WA, USA 2002–2020). The single-beam echosounder was fitted with a 204.8 kHz–8.3° beam width transducer. Our plant detection settings within Visual Aquatic were set to a plant detection threshold of −60 dB, a plant detection length criterion of 25 cm, and a maximum plant depth of 10 m. These settings were found to result in plausible mappings for macrophyte presence within our study region. The data were used to evaluate how well the HSS and individual model inputs correlate with actual macrophyte occurrence. To do this, we converted the presence and absence of data into probabilities of occurrence relative to the model inputs or HSS. In practical terms, this involved calculating the ratio of presence to absence measurements for each value of the HSS or the model parameters.

3. Results

After outlining our methodology, we present our results, including the macrophyte occurrence in correspondence to the model inputs and the macrophyte habitat suitability in the Osterseen Lake District.

3.1. Model Input and Macrophyte Occurrence

To provide insight into the relation of the model inputs to actual habitats, presence and absence data from hydroacoustic macrophyte mappings were used. The relationships between macrophyte occurrence probability and each of the four abiotic predictors are presented in Figure 6. Macrophytes predominantly occurred in the lower ranges of 1–10% PAR availability. A significant negative correlation was observed between PAR availability and macrophyte occurrence probability, with a Pearson correlation coefficient of r = −0.45 (Appendix A: Table A1). The littoral slope appears to have little linear influence on macrophyte occurrence, but distance correlation analysis [74,75] suggests significant non-linear correlation ($\mathcal{R}$ = 0.41, p-value$_{dcor}$ = 0.003, Appendix A: Table A1). A maximum macrophyte occurrence probability (0.4) is observed at around 10° of the littoral slope, which decreases toward gentler and steeper slopes. Contrarily, both the distance to the nearest groundwater inflow and the water depth, showed significant linear negative correlations with macrophyte occurrence probability (Pearson's r = −0.53 and −0.68, $p < 0.001$, Appendix A: Table A1). Distance correlation analysis indicated an especially high correlation for depth ($\mathcal{R}$ = 0.757, p-value$_{dcor} < 0.001$, Appendix A: Table A1). The probability of macrophyte occurrence decreases with increasing distance from the groundwater inflow. Water depth shows a peak in the probability of occurrence at about 3–4 m depth. The probability then decreases on both sides. At about 10 m depth, macrophyte occurrence is unlikely.

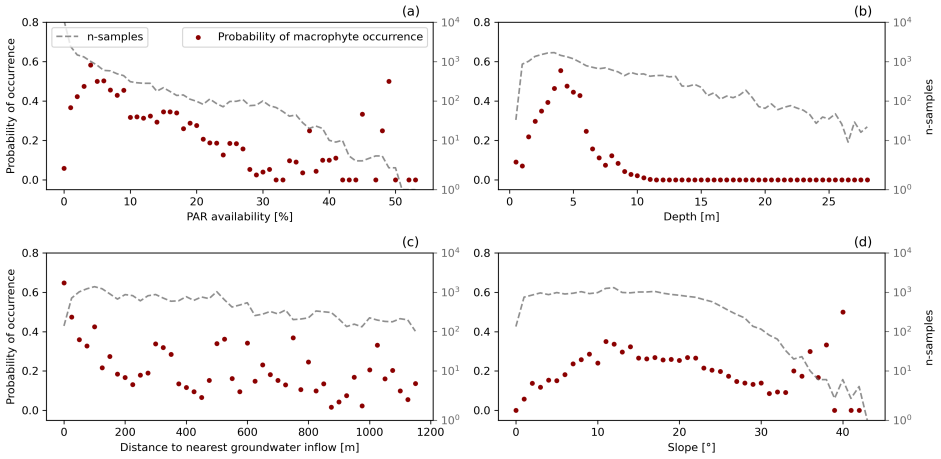

Figure 6. Comparison between the probability of macrophyte occurrence based on sonar mappings and abiotic predictors: (**a**) PAR availability, (**b**) water depth, (**c**) distance to the nearest groundwater inflow, and (**d**) littoral slope.

3.2. Model

The HSM result is represented by the habitat suitability score (HSS), modeled over the growing season 2023 (May to September), ranging between 0 and 100. The HSS was compared with in situ hydroacoustic mappings representing actual habitats, as depicted in Figure 7. Our modeled HSS and the actual habitats strongly correlate with Pearson's r = 0.908 (n = 24,073). This robust correlation indicates that the HSS is a suitable measure for assessing potential habitats within our study region. The fitted function allows us to interpret the HSS in terms of probability of occurrence.

The probability of occurrence was used to pinpoint sensible thresholds for high, medium, and low habitat suitability within the HSS. Figure 7 reveals that for an HSS above 67.1, the probability of occurrence (>50%) exceeds the probability of absence. This means it is more likely for macrophytes to be present in habitats with HSS > 67.1 than to be absent. Therefore we used this threshold to identify highly suitable macrophyte habitats. Additionally, we also included an HSS threshold for medium habitat suitability (HSS > 54.7), which translates to a probability of macrophyte occurrence greater than 33% (see Figure 7). An HSS < 54.7 would be interpreted as having a low habitat suitability. Figure 8 presents the

habitat suitability in the Osterseen lakes, categorized as low, medium, or high, based on the corresponding probability of macrophyte occurrence (low > 33%, medium = 33–50%, and high > 50%). Due to a lack of sufficient valid pixels for determining K_dPAR, the lakes WS, FKS, and FOS were excluded from the model. More detailed representations of the modeled habitat suitability, along with sonar macrophyte presence and absence, are depicted in Figure 9. These maps allow us to identify regions of high macrophyte habitat suitability and those with low habitat suitability.

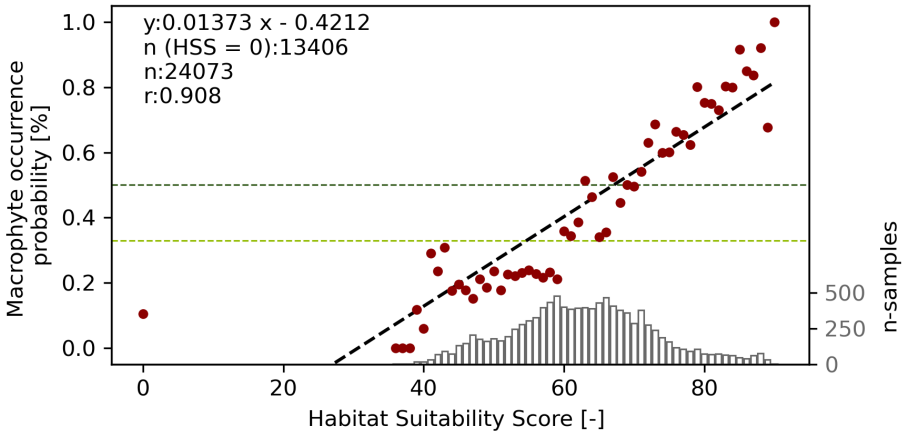

Figure 7. Scatter correlation plot between the modeled habitat suitability score (HSS) and macrophyte occurrence probability from sonar mappings. The horizontal dotted lines indicate macrophyte occurrence of 33% and 50%, respectively.

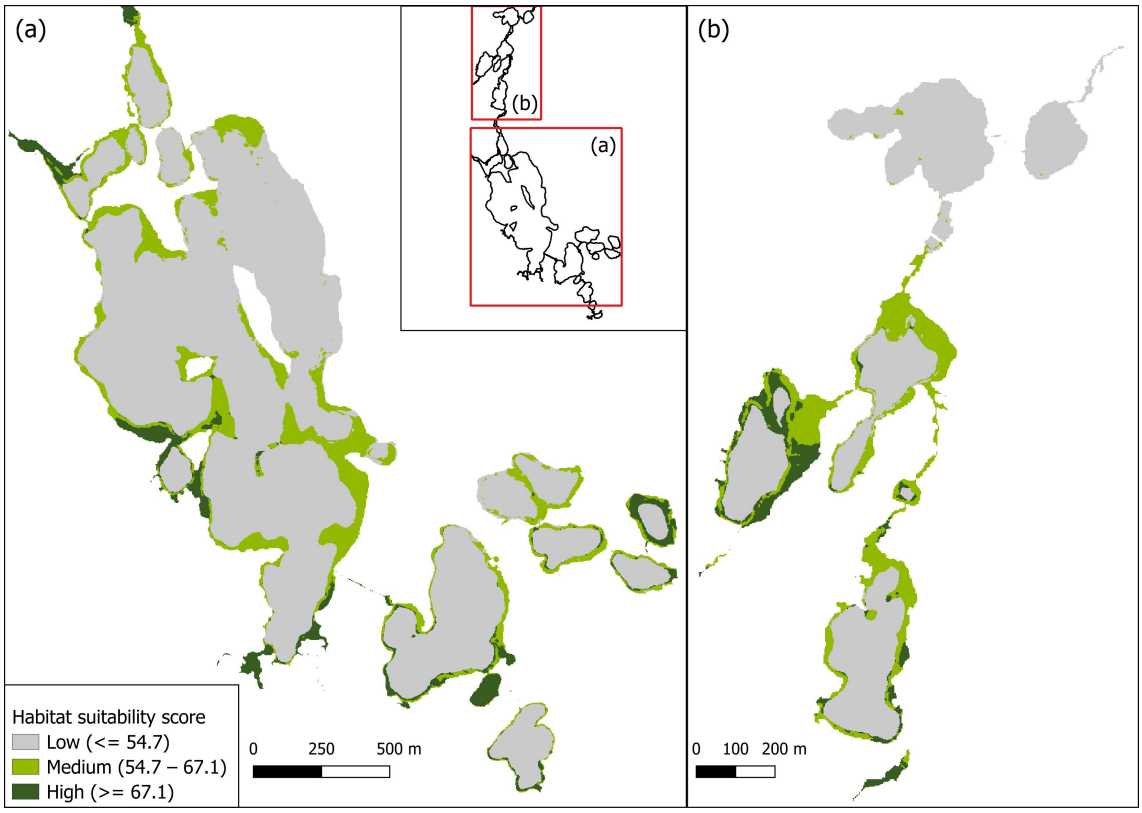

Figure 8. Modeled habitat suitability for macrophytes in 2023. (**a**) Central, southern, and eastern lakes, (**b**) northern lakes.

Overall, Figure 8 reveals distinct spatial variations in habitat suitability. Areas with high habitat suitability were predominantly concentrated in the moderately shallow regions near areas with groundwater inflows. According to the modeled HSS, the two northern lakes, US and GAS, the central lakes, AS and OBS, as well as the eastern half of the lake OS are rather unsuitable macrophyte habitats. These locations are considerably distant from groundwater inflows.

Figure 9 shows more detailed views of areas of high potential habitat suitability, along with the tracks of the hydroacoustic macrophyte habitat mapping. Figure 9b,c show examples in Lake WBS and Lake FKS where modeled potential habitats align well with the patterns of the actual habitats. In contrast, in Figure 9a,d, the potential habitats differ from actual habitats.

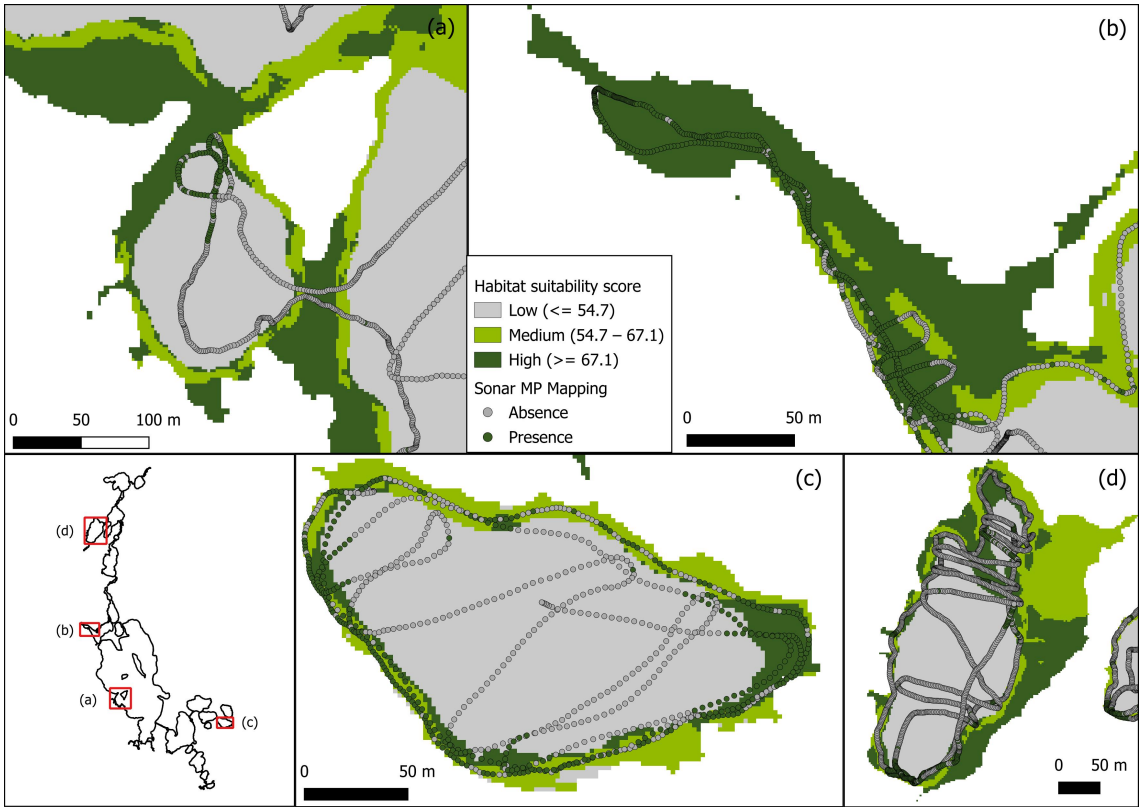

Figure 9. Modeled habitat suitability for 2023 and the actual presence of macrophytes as measured with hydroacoustic mappings. (**a**) Western Bay of Lake Großer Ostersee (OS), (**b**) Shallow side-arm of Lake Westlicher Breitenauersee (WBS), (**c**) Lake Fischkaltersee (FKS), and (**d**) Lake Lustsee (LS).

4. Discussion

After presenting our results, we will interpret them in the following section. The aim of our study was to establish the potential habitat of macrophytes based on abiotic predictors, providing a practical tool for decision-makers and water resource managers, and illustrating the added value of remote sensing for modeling and monitoring in freshwater environments. Therefore, we will discuss the selected habitat predictors, consider their impact on habitat selection, and identify additional abiotic and biotic predictors that could explain the differences between the modeled potential and actual habitats. Then we will evaluate the integration of remotely sensed data into the HSM and examine the potential role of an HSM with remotely sensed data as a tool for water management.

4.1. Habitat Predictors

The HSM evaluates habitat suitability based on four abiotic predictors: the availability of PAR, littoral slope, water depth, and distance to groundwater inflows. These factors account for the spatial and temporal patterns observed within our score.

Each lake showed littoral areas where the requirements for PAR availability were met (Figure 5a). The availability of PAR depends on the water depth, K_dPAR, irradiance geometry, and irradiance; therefore, the results are related. Clear lakes with low K_dPAR, such as Lake LS, exhibit relatively large depths that remain above the PAR threshold, reaching a maximum of approximately 5 m. In contrast, lakes with higher K_dPAR, such as Lake GS and US, have their maximum growing depths above the PAR threshold at around 4 m during the mean growing season. This can be attributed to the higher attenuation by humic acids in the water of the northern lakes. South-facing littoral slopes generally show higher PAR availability compared to north-facing slopes; however, the differences are small since refraction dampens these effects. Overall, the availability of PAR limits habitable zones to littoral areas and shallow banks. A pixel's suitability is further influenced by both littoral slope and water depth on a small scale (<50 m), while on a larger scale (>50 m), the proximity to the nearest groundwater inflow appears to determine favorable regions.

Our analysis of viable habitats for macrophytes seems to be largely plausible as evidenced by high correlations in Figure 7. In single cases, the model underestimates habitat suitability (Figure 9a); only in Lake LS does the model overestimate the habitat suitability compared to actual macrophyte occurrence (Figure 9d).

We found that macrophytes appear to prefer the environmental conditions provided by greater water depths rather than the higher availability of PAR in the shallow littoral (Figure 6). We suspect that cooler water temperatures and stronger stratification may contribute to this observation.

The low PAR availabilities under which we observed macrophytes in our study area were particularly notable. Middelboe and Markager [56] described a general threshold of 5.1% (corrected for 3% albedo) as the average minimum light availability requirement for charophytes and caulescent angiosperms. Using remotely sensed PAR, we found this to be the mean PAR availability under which macrophytes were observed in our study region (Table A1); the 25% quantile of PAR availability values with macrophyte occurrence served as the minimum threshold for PAR requirements, i.e., 1.3%. Middelboe and Markager [56] reported similar ranges of surface irradiance at maximum growing depth averaged from multiple studies. Some differences, however, are observed between the PAR availability presented in this study and the surface irradiance at maximum growing depth by Middelboe and Markager [56]. These differences can be attributed to the use of irradiance geometry in calculating PAR availability. Furthermore, we considered average K_dPAR values for each lake, which introduce uncertainties due to possible spatial variability. Near groundwater inflows, the local K_dPAR could be lower than the lake average due to the inflow of clear water, resulting in higher PAR values being available at the depths where macrophytes are growing. This phenomenon may also explain incorrectly underestimated habitat conditions in Figure 9a. Nonetheless, it is useful to work with average K_dPAR values for each lake, as it can only be retrieved in optically deep water, of which there are few valid pixels in each lake. The alternative to using directly retrieved remotely sensed K_dPAR from the MSI data would introduce noise as well as spatial and temporal gaps in the HSM.

Unexpectedly, the littoral slope had a non-linear correlation to the occurrence of macrophytes (Figure 6 and Table A1). Macrophyte occurrence in relationship to the littoral slope seemed to form an optimum curve that peaks around a 10° slope (Figure 6). Thus, the data from our small lakes did not entirely support the general assumption made by previous models where macrophyte habitat suitability declines with increasing slope angles. For instance, Fleming et al. [57] selected slope as a primary predictor for potential macrophyte habitats within their study region. Steep

slopes are known to have a negative impact on plant biomass [37,69], suggesting poorer growing conditions at steeper slopes. However, moderate littoral slopes could offer more suitable habitats than gentle slopes due to better exposure to the sun and, therefore, higher PAR availability.

The probability of macrophyte occurrence showed a significant negative linear correlation (Pearson's r = −0.532) with our study-specific predictor, i.e., the distance to the nearest groundwater inflow (Table A1). Short distances to groundwater inflows seem to favor macrophyte presence, while large distances appear to limit viable habitats. We suspect that the cold inflow of groundwater during the summer and the reduced attenuation of PAR near these inflows facilitate macrophyte occurrence. Additionally, nutrients could be locally introduced through the groundwater inflow.

When aggregated into the HSS score, these predictors showed a Pearson correlation of r = 0.908 with the habitat preferences of freshwater macrophytes in the Lake District.

4.2. Modeled Potential Habitats vs. Actual Habitats

Modeled potential habitats and actually measured habitats overlap in most cases. However, there are a few locations where the two differ. This was at least partially expected due to the fallacious absences, referring to the absence of a species even when the habitat requirements are met. Such absences can be caused by the limited dispersal of a species, local extinction, patch sizes too small to host a viable population, or biotic interactions such as competition or succession stages. These cases are inevitable simplifications when modeling habitats [53].

Apart from fallacious absences, additional abiotic factors could play a role. A commonly used predictor not considered in this study is wind and wave fetch [54,57,76,77]. Strong winds or waves can dislodge plants and increase suspended sediment concentrations, which impact light availability [57]. Compared to the lakes investigated by Hudon et al. [54], Fleming et al. [57], and Tang et al. [77], the lakes in our study are relatively small. Wind and fetch hardly develop waves, so this process might not significantly affect the macrophytes. Another possible abiotic input into an HSM could involve the chemical and physical properties of the lake water and the sediment. Harrow-Lyle and Kirkwood [78] identified the availability of nutrients, such as sodium, magnesium, and potassium, as important factors for the habitat preferences of *Nitellopsis obtusa*. Rey-Boissezon and Auderset Joye [79] found that water conductivity helped discriminate the habitat preferences of Charophyte species. Bornette and Puijalon [55] stated that dissolved carbon, nitrogen, and phosphorous are the driving nutrients for aquatic plant life. Their availability cannot only limit the presence or absence but also influence species richness.

Other than abiotic factors, biotic factors also control the actual occurrence of macrophytes. Carps, present in the Lake District, are known to feed on macrophytes and cause uprooting and disturbance through their feeding behavior, negatively affecting both abundance and biomass [80,81]. Additionally, the growth of periphyton, which can colonize macrophytes, was found to attenuate up to 80% of light in experiments in the Osterseen Lake District [51] This can, consequently, limit the macrophyte abundance as well. These biotic factors cannot be included in abiotic models such as the one used in this study, and should, therefore, be considered when drawing conclusions from modeled potential habitats to actual habitats.

In summary, despite the uncertainties inherent in potential habitat suitability modeling, our study successfully developed a robust model that effectively explains the majority of macrophyte presences and absences. Users, however, should be aware of the potential uncertainties when modeling potential habitats and relating them to actual habitats.

4.3. Employing Remote Sensing in Habitat Modeling and Monitoring

Having demonstrated that remotely sensed data can be used in habitat suitability modeling, we will discuss the benefits and implications of its further use.

Remote sensing offers a multitude of use cases but is generally regarded primarily as a source of data. In limnological settings, remote sensing can provide information on water transparency (dissolved organic carbon, turbidity, Secchi depth), biotic properties (algal blooms, phenology, species composition), hydrology (water level and bathymetry), as well as temperature and ice cover [82]. Remote sensing applications in lake research are increasing. Nevertheless, only 9% of the studies on climate-related shifts regarding lake ecosystems involve remote sensing data [83].

In our study, we used Sentinel-2 MSI data to assess PAR availability, complementing an existing in situ dataset across spatial, temporal, and quantitative dimensions. We used 139 MSI scenes to introduce a temporal dimension to the HSM that would not have been available otherwise. The time series allows us to monitor the PAR availability over an entire growing season or even an entire year to develop an HSM. This approach offers valuable insights into temporal light dynamics. For instance, Figure A1 demonstrates monthly variations, revealing two interesting effects. PAR availabilities of above 100% occur at the lake bottom during the winter months. This is caused by low sun zenith angles, when incoming radiation is refracted below the water surface to higher angles, leading to higher PAR availabilities at the lake bottom depth than above the water surface. The other observable effect is how light attenuation and the zenith angle compete against each other in the penetration depth of light, resulting in a maximum penetration depth in May. Analyses such as these, if done in situ, would be labor- and cost-intensive and limited to single measurement locations. Remote sensing allows us to efficiently gather a large dataset, with in situ data only required for quality control.

Nevertheless, using remotely sensed data presents its own set of challenges. Cloud coverage hindered retrieving K_dPAR data for every lake, during each month, as depicted in Figure 4. Apart from cloud cover, we encountered typical constraints inherent in optical water remote sensing applications. These included the need to correct for or flag out pixels affected by sun glint, adjacency effects, and instances where existing atmospheric correction algorithms may prove insufficient. These challenges demand a comprehensive understanding of remote sensing and often deter inexperienced users from considering its application in water monitoring [84]. As the demand for ready-to-use products increases, the availability of ready-made datasets for the assessment of water parameters derived from remotely sensed data also tends to increase. One example is the extensive open-access catalog of reprocessed remote sensing products from the Copernicus Marine Service CMEMS (https://data.marine.copernicus.eu/products, accessed on 2 March 2024). Remotely sensed products are also becoming more readily available for inland water applications, such as the water datasets from the Copernicus Global Land Operations Service CGLOPS (https://land.copernicus.eu/global/, accessed on 2 March 2024) or the data acquired for lakes in the ESA Climate Change initiative CCI-lakes (https://climate.esa.int/en/projects/lakes/, accessed on 2 March 2024). This trend is extending the benefits of remote sensing to a wider user base.

In summary, integrating remote sensing data into an HSM facilitates the expansion of the model across multiple dimensions, as shown in this study. Additionally, it offers a cost and time-efficient way to gather various key water parameters in near real-time.

4.4. GIS and Remote Sensing-Supported HSMs as Tools for Water Management

Finally, we explore the tangible applications of GIS and remote sensing-supported HSMs in water management, highlighting their practical utility and relevance in real-world scenarios.

It is not entirely novel to support HSMs designed for water resource management purposes, such as macrophyte re-establishment projects, with GIS data [57]. The simplicity of linear-weighted GIS models, such as the one presented in this study, allows users to easily recreate them on their own or expand them. Due to their straightforward nature and lack of fitting to specific datasets, these models are expected to be more transferable

than statistical models [85]. Therefore, such HSMs could serve as valuable tools for water resource planning and regulation efforts.

The novelty of our research lies in the addition of remote sensing data and the derivation of PAR availability from the data, introducing a temporal dimension to our model. Therefore, the model may be used to monitor changing macrophyte habitats over time. Global losses in aquatic vegetation are observed [18], driven by changes in climate and land use. Furthermore, global warming appears to drive local changes, such as *Chara* spp. continuing to exhibit wintergreen in Germany or the increased frequency of observations of invasive *Najas intermedia* in Germany [86]. Temporal HSMs can monitor how habitat distribution responds to change and can predict potential habitat distribution for future scenarios. Rising water levels, changes in trophic state, or changes in morphology could be simulated with such models to plan how habitats will respond to water management measures. This could help manage uncertainties in environmental planning and aid decision-making [24]. A further potential use case could be the monitoring of invasive species' habitats. Potential habitats for invasive macrophytes are predicted to increase in the northern hemisphere [19]. Florêncio et al. [69] demonstrated how the habitat preferences of the invasive macrophyte *Hydrillyla verticillata* differed from the habitat preferences of the native macrophyte *Egeria najas*. HSMs could leverage these differences to identify habitats at risk of species invasion [24,87]. Another potential application could involve identifying areas for habitat conservation or for re-establishing ecosystems. Habitats of species facing significant threats of extinction can be pinpointed using HSMs and then evaluated for protective measures [24]. We firmly believe that developing species-specific models is a crucial step toward more effective HSMs for management purposes. They could help in understanding climate change-driven shifts in species composition and displacements of one species by another. Such a model would require extensive knowledge about the species-specific habitat requirements, either through experiments or derived from presence and absence data. Remote sensing data could play a pivotal role in this, especially if in situ data are sparse.

In essence, GIS and remote sensing-supported HSMs offer a straightforward yet powerful approach to monitoring habitats under changing conditions, providing both versatility and transparency. Their ability to map habitats in present and future scenarios makes them promising tools for addressing ecological challenges and guiding decision-making processes.

5. Conclusions

In this study, we explored the practical application of GIS and remote sensing-supported HSMs to analyze the potential habitat of freshwater macrophytes in water management, highlighting their utility in real-world scenarios. While using GIS data to support HSMs for water resource management is not new, our study introduced the novelty of integrating remote sensing data, adding a temporal dimension to HSMs built for a series of small lakes in the Lake Osterseen District (Germany). We were able to determine the potential habitats of macrophytes in our lake system. We identified PAR availability derived from Sentinel-2 MSI data, the distance to the nearest groundwater inflow, the water depth, and the littoral slope as suitable predictors of potential macrophyte habitats. These remote sensing-supported temporal HSMs can monitor and predict changes in macrophyte habitats during a growing season, but also in response to global and local environmental changes. They can also be used to monitor invasive species habitats and identify areas for conservation or ecosystem re-establishment and are therefore a practical tool for decision-makers. For a better understanding of habitat requirements, we see the development of species-specific models as a crucial step toward more effective HSMs, especially when combined with remote sensing data. In essence, GIS and remote sensing-supported HSMs offer a versatile and transparent approach to monitor and predict habitats under changing conditions, aiding in ecological challenges and decision-making processes.

Author Contributions: Conceptualization, T.S. and N.O.; methodology, B.R.; software, B.R. and F.K.; validation, B.R.; formal analysis, B.R. and F.K.; investigation, B.R., F.K. and T.S.; resources, N.O.; data curation, B.R., F.K. and T.S.; writing—original draft preparation, B.R. and F.K.; writing—review and editing, F.K., K.K., T.S. and N.O.; visualization, B.R. and F.K.; supervision, N.O.; project administration, T.S. and N.O.; funding acquisition, N.O. All authors have read and agreed to the published version of the manuscript.

Funding: This research was funded by the Deutsche Forschungsgemeinschaft (DFG, German Research Foundation) grant number 496344580.

Data Availability Statement: The raw data supporting the conclusions of this article will be made available by the authors on request.

Acknowledgments: We are grateful to the Limnological Research Station Iffeldorf, a part of the Department of Ecology and Ecosystem Management at the Technical University of Munich, for hosting us during our field campaign and for their collaboration on this project. We would also like to thank LfU for providing us with their bathymetric sonar mappings. Special acknowledgment goes to Quinten Vanhellemont for his invaluable assistance and for his contribution to implementing an irradiance-approximation function for us in ACOLITE.

Conflicts of Interest: The authors declare no conflicts of interest. The funders had no role in the design of the study; in the collection, analyses, or interpretation of data; in the writing of the manuscript; or in the decision to publish the results.

Abbreviations

The following abbreviations are used in this manuscript:

HSM	habitat suitability model
PAR	photosynthetically active radiation
K_dPAR	diffuse attenuation coefficient for photosynthetically active radiation
$E_d(\lambda)$	downwelling direct solar irradiance at wavelength λ
HSS	habitat suitability score

Appendix A

Table A1. The statistical evaluation of abiotic predictors of macrophyte occurrences. Pearson correlation coefficient r and p-value, and distance correlation coefficient $\mathcal{R}$ and p-value$_{dcor}$ were calculated based on the probability of occurrence from Figure 6.

	%PAR	**Slope**	**Distance to Inflow**	**Depth**
count	5637.0	6276.0	6509.0	6509.0
mean	5.21	13.33	293.95	3.85
std	5.68	6.39	267.55	1.56
min	0.0	0.66	0.88	0.35
25%	1.3	8.64	84.08	2.75
50%	3.53	12.52	198.52	3.75
75%	6.92	17.81	492.31	4.78
max	50.7	42.62	1150.76	10.8
r	−0.445	0.131	−0.532	−0.678
p-value	0.001	0.397	0.0	0.0
$\mathcal{R}$	0.676	0.41	0.486	0.757
p-value$_{dcor}$	0.0	0.003	0.0	0.0

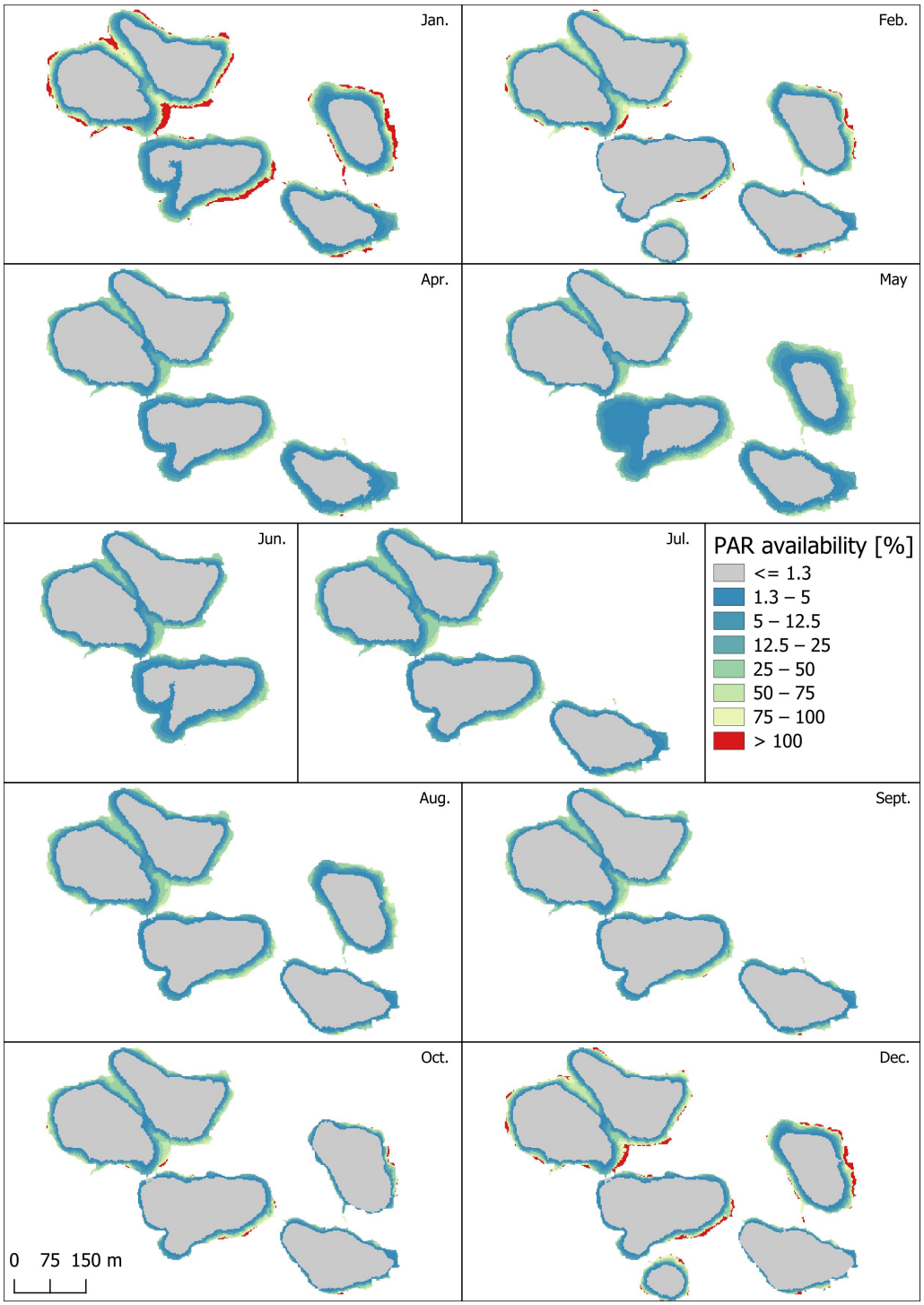

Figure A1. Mapped mean PAR availability in the % of the above surface PAR at the bottom depth for the eastern lake cluster (ES, BS, FOS, FKS, and HS).

References

1. Dudgeon, D.; Arthington, A.H.; Gessner, M.O.; Kawabata, Z.I.; Knowler, D.J.; Lévêque, C.; Naiman, R.J.; Prieur-Richard, A.H.; Soto, D.; Stiassny, M.L.J.; et al. Freshwater biodiversity: Importance, threats, status and conservation challenges. *Biol. Rev.* **2006**, *81*, 163–182. [CrossRef] [PubMed]
2. Reid, A.J.; Carlson, A.K.; Creed, I.F.; Eliason, E.J.; Gell, P.A.; Johnson, P.T.J.; Kidd, K.A.; MacCormack, T.J.; Olden, J.D.; Ormerod, S.J.; et al. Emerging threats and persistent conservation challenges for freshwater biodiversity. *Biol. Rev.* **2019**, *94*, 849–873. [CrossRef] [PubMed]
3. Adrian, R.; O'Reilly, C.M.; Zagarese, H.; Baines, S.B.; Hessen, D.O.; Keller, W.; Livingstone, D.M.; Sommaruga, R.; Straile, D.; Van Donk, E.; et al. Lakes as sentinels of climate change. *Limnol. Oceanogr.* **2009**, *54*, 2283–2297. [CrossRef] [PubMed]

4. Loewen, C. Lakes as model systems for understanding global change. *Nat. Clim. Chang.* **2023**, *13*, 304–306. [CrossRef]
5. Dayton, P.K. Toward an understanding of community resilience and the potential effects of enrichments to the benthos at McMurdo Sound, Antarctica. In *Proceedings of the Colloquium on Conservation Problems in Antarctica*; Allen Press: Lawrence, KS, USA, 1972; pp. 81–96.
6. Cook, C.D.K.; Gut, B.J.; Rix, E.M.; Schneller, J. *Water Plants of the World: A Manual for the Identification of the Genera of Freshwater Macrophytes*; Springer Science & Business Media: The Hague, The Netherlands, 1974.
7. Carpenter, S.R.; Lodge, D.M. Effects of submersed macrophytes on ecosystem processes. *Aquat. Bot.* **1986**, *26*, 341–370. [CrossRef]
8. Pieczyńska, E. Detritus and nutrient dynamics in the shore zone of lakes: A review. *Hydrobiologia* **1993**, *251*, 49–58. [CrossRef]
9. Finkler Ferreira, T.; Crossetti, L.O.; Motta Marques, D.M.L.; Cardoso, L.; Fragoso, C.R.; van Nes, E.H. The structuring role of submerged macrophytes in a large subtropical shallow lake: Clear effects on water chemistry and phytoplankton structure community along a vegetated-pelagic gradient. *Limnologica* **2018**, *69*, 142–154. [CrossRef]
10. Bolduc, P.; Bertolo, A.; Bernadette, P.A. Does submerged aquatic vegetation shape zooplankton community structure and functional diversity? A test with a shallow fluvial lake system. *Hydrobiologia* **2016**, *778*, 151–165. [CrossRef]
11. Deosti, S.; Bomfim, F.; Lansac-Tôha, F.; Quirino, B.; Bonecker, C.; Lansac-Tôha, F. Zooplankton taxonomic and functional structure is determined by macrophytes and fish predation in a Neotropical river. *Hydrobiologia* **2021**, *848*, 1–16. [CrossRef]
12. Emery-Butcher, H.E.; Beatty, S.J.; Robson, B.J. The impacts of invasive ecosystem engineers in freshwaters: A review. *Freshw. Biol.* **2020**, *65*, 999–1015. [CrossRef]
13. Jones, C.G.; Lawton, J.H.; Shachak, M. Organisms as Ecosystem Engineers. *Oikos* **1994**, *69*, 373–386. [CrossRef]
14. Thomaz, S.M.; Cunha, E.R.d. The role of macrophytes in habitat structuring in aquatic ecosystems: Methods of measurement, causes and consequences on animal assemblages' composition and biodiversity. *Acta Limnol. Bras.* **2010**, *22*, 218–236. [CrossRef]
15. Bakker, E.S.; Wood, K.A.; Pagès, J.F.; Veen, G.F.C.; Christianen, M.J.A.; Santamaría, L.; Nolet, B.A.; Hilt, S. Herbivory on freshwater and marine macrophytes: A review and perspective. *Aquat. Bot.* **2016**, *135*, 18–36. [CrossRef]
16. Wolters, J.W.; Verdonschot, R.C.M.; Schoelynck, J.; Brion, N.; Verdonschot, P.F.M.; Meire, P. Stable isotope measurements confirm consumption of submerged macrophytes by macroinvertebrate and fish taxa. *Aquat. Ecol.* **2018**, *52*, 269–280. [CrossRef]
17. Thomaz, S.M. Ecosystem services provided by freshwater macrophytes. *Hydrobiologia* **2023**, *850*, 2757–2777. [CrossRef]
18. Zhang, Y.; Jeppesen, E.; Liu, X.; Qin, B.; Shi, K.; Zhou, Y.; Thomaz, S.M.; Deng, J. Global loss of aquatic vegetation in lakes. *Earth-Sci. Rev.* **2017**, *173*, 259–265. [CrossRef]
19. Lind, L.; Eckstein, R.L.; Relyea, R.A. Direct and indirect effects of climate change on distribution and community composition of macrophytes in lentic systems. *Biol. Rev.* **2022**, *97*, 1677–1690. [CrossRef] [PubMed]
20. Kirk, J.T.O. *Light and Photosynthesis in Aquatic Ecosystems*, 3rd ed.; Cambridge University Press: Cambridge, UK, 2010. [CrossRef]
21. Mooij, W.M.; Janse, J.H.; De Senerpont Domis, L.N.; Hülsmann, S.; Ibelings, B.W. Predicting the effect of climate change on temperate shallow lakes with the ecosystem model PCLake. In *Shallow Lakes in a Changing World*; Gulati, R.D., Lammens, E., De Pauw, N., Van Donk, E., Eds.; Springer: Dordrecht, The Netherlands, 2007; pp. 443–454. [CrossRef]
22. European Environment Agency. *European Rivers and Lakes: Assessment of Their Environmental State*; Number 1 in EEA environmental monographs; European Environmental Agency: Copenhagen, Denmark, 1994.
23. Elith, J.; Leathwick, J. Species Distribution Models: Ecological Explanation and Prediction Across Space and Time. *Annu. Rev. Ecol. Evol. Syst.* **2009**, *40*, 677–697. [CrossRef]
24. Guisan, A.; Tingley, R.; Baumgartner, J.B.; Naujokaitis-Lewis, I.; Sutcliffe, P.R.; Tulloch, A.I.T.; Regan, T.J.; Brotons, L.; McDonald-Madden, E.; Mantyka-Pringle, C.; et al. Predicting species distributions for conservation decisions. *Ecol. Lett.* **2013**, *16*, 1424–1435. [CrossRef]
25. Warren, D.L.; Matzke, N.J.; Iglesias, T.L. Evaluating presence-only species distribution models with discrimination accuracy is uninformative for many applications. *J. Biogeogr.* **2020**, *47*, 167–180. [CrossRef]
26. Barnes, M.A.; Jerde, C.L.; Wittmann, M.E.; Chadderton, W.L.; Ding, J.; Zhang, J.; Purcell, M.F.; Budhathoki, M.; Lodge, D.M. Geographic selection bias of occurrence data influences transferability of invasive *Hydrilla verticillata* distribution models. *Ecol. Evol.* **2014**, *4*, 2584–2593. [CrossRef] [PubMed]
27. Lee-Yaw, J.; McCune, J.; Pironon, S.; Sheth, S. Species distribution models rarely predict the biology of real populations. *Ecography* **2021**, *2022*, e05877. [CrossRef]
28. Araújo, M.B.; Guisan, A. Five (or so) challenges for species distribution modelling. *J. Biogeogr.* **2006**, *33*, 1677–1688. [CrossRef]
29. Kellner, C.J.; Brawn, J.D.; Karr, J.R. What Is Habitat Suitability and how Should it be Measured? In *Wildlife 2001: Populations*; McCullough, D.R., Barrett, R.H., Eds.; Springer: Dordrecht, The Netherlands, 1992; pp. 476–488. [CrossRef]
30. Peterson, A.; Soberón, J. Species Distribution Modeling and Ecological Niche Modeling: Getting the Concepts Right. *Nat. Conserv.* **2012**, *10*, 1–6. [CrossRef]
31. Melo-Merino, S.M.; Reyes-Bonilla, H.; Lira-Noriega, A. Ecological niche models and species distribution models in marine environments: A literature review and spatial analysis of evidence. *Ecol. Model.* **2020**, *415*, 108837. [CrossRef]
32. McGill, B.J. Ecology. Matters of scale. *Science* **2010**, *328*, 575–576. [CrossRef] [PubMed]
33. Alahuhta, J. Geographic patterns of lake macrophyte communities and species richness at regional scale. *J. Veg. Sci.* **2015**, *26*, 564–575. [CrossRef]
34. Scheffer, M.; Hosper, S.; Meijer, M.L.; Moss, B.; Jeppesen, E. Alternative equilibria in shallow lakes. *Trends Ecol. Evol.* **1993**, *8*, 275–279. [CrossRef]

35. Stefanidis, K.; Sarika, M.; Papastegiadou, E. Exploring environmental predictors of aquatic macrophytes in water-dependent Natura 2000 sites of high conservation value: Results from a long-term study of macrophytes in Greek lakes. *Aquat. Conserv. Mar. Freshw. Ecosyst.* **2019**, *29*, 1133–1148. [CrossRef]
36. Van Echelpoel, W.; Goethals, P.L.M. Variable importance for sustaining macrophyte presence via random forests: Data imputation and model settings. *Sci. Rep.* **2018**, *8*, 14557. [CrossRef]
37. Duarte, C.M.; Kalff, J. Littoral slope as a predictor of the maximum biomass of submerged macrophyte communities1,1: Submerged macrophyte biomass. *Limnol. Oceanogr.* **1986**, *31*, 1072–1080. [CrossRef]
38. He, L.; Zhu, T.; Wu, Y.; Li, W.; Zhang, H.; Zhang, X.; Cao, T.; Ni, L.; Hilt, S. Littoral Slope, Water Depth and Alternative Response Strategies to Light Attenuation Shape the Distribution of Submerged Macrophytes in a Mesotrophic Lake. *Front. Plant Sci.* **2019**, *10*, 169. [CrossRef] [PubMed]
39. Lewerentz, A.; Hoffmann, M.; Sarmento Cabral, J. Depth diversity gradients of macrophytes: Shape, drivers, and recent shifts. *Ecol. Evol.* **2021**, *11*, 13830–13845. [CrossRef] [PubMed]
40. Søndergaard, M.; Phillips, G.; Hellsten, S.; Kolada, A.; Ecke, F.; Mäemets, H.; Mjelde, M.; Azzella, M.M.; Oggioni, A. Maximum growing depth of submerged macrophytes in European lakes. *Hydrobiologia* **2013**, *704*, 165–177. [CrossRef]
41. Alahuhta, J.; Lindholm, M.; Baastrup-Spohr, L.; García Girón, J.; Toivanen, M.; Heino, J.; Murphy, K. Macroecology of macrophytes in the freshwater realm: Patterns, mechanisms and implications. *Aquat. Bot.* **2021**, *168*, 103325. [CrossRef]
42. Johnson, R.K.; Toprak, V. Local habitat is a strong determinant of spatial and temporal patterns of macrophyte diversity and composition in boreal lakes. *Freshw. Biol.* **2021**, *66*, 1490–1501. [CrossRef]
43. García-Girón, J.; Heino, J.; García-Criado, F.; Fernández-Aláez, C.; Alahuhta, J. Biotic interactions hold the key to understanding metacommunity organisation. *Ecography* **2020**, *43*, 1180–1190. [CrossRef]
44. Crane, K.; Kregting, L.; Coughlan, N.E.; Cuthbert, R.N.; Ricciardi, A.; MacIsaac, H.J.; Dick, J.T.; Reid, N. Abiotic and biotic correlates of the occurrence, extent and cover of invasive aquatic Elodea nuttallii. *Freshw. Biol.* **2022**, *67*, 1559–1570. [CrossRef] [PubMed]
45. Williams, A.E.; Moss, B.; Eaton, J. Fish induced macrophyte loss in shallow lakes: Top–down and bottom–up processes in mesocosm experiments. *Freshw. Biol.* **2002**, *47*, 2216–2232. [CrossRef]
46. Nechad, B.; Ruddick, K. A model of diffuse attenuation of the downwelling irradiance for ecosystem models. In Proceedings of the SPIE Asia-Pacific Remote Sensing, Incheon, Republic of Korea, 3 November 2010; p. 78580D. [CrossRef]
47. Deutscher Wetterdienst (German Weather Service). Climate Data Center (CDC): Grids of Multi-Annual Mean Precipitation Height for Germany, Versionv21.3, 2017. Location: Iffeldorf, 2021. Available online: https://cdc.dwd.de/portal/ (accessed on 19 April 2024).
48. Deutscher Wetterdienst (German Weather Service). Climate Data Center (CDC): Weather Station Data of Multi-Annual Mean Temperature, Location: Attenkam, 2020. Available online: https://cdc.dwd.de/portal/ (accessed on 19 April 2024).
49. Gruenert, U.; Raeder, U. Growth responses of the calcite-loricated freshwater phytoflagellate *Phacotus lenticularis* (Chlorophyta) to the $CaCO_3$ saturation state and meteorological changes. *J. Plankton Res.* **2014**, *36*, 630–640. [CrossRef]
50. Zwirglmaier, K.; Keiz, K.; Engel, M.; Geist, J.; Raeder, U. Seasonal and spatial patterns of microbial diversity along a trophic gradient in the interconnected lakes of the Osterseen Lake District, Bavaria. *Front. Microbiol.* **2015**, *6*, 1168. [CrossRef] [PubMed]
51. Raeder, U.; Ruzicka, J.; Goos, C. Characterization of the light attenuation by periphyton in lakes of different trophic state. *Limnologica* **2010**, *40*, 40–46. [CrossRef]
52. Melzer, A. Aquatic macrophytes as tools for lake management. *Hydrobiologia* **1999**, *395*, 181–190. [CrossRef]
53. Hirzel, A.H.; Le Lay, G. Habitat suitability modelling and niche theory. *J. Appl. Ecol.* **2008**, *45*, 1372–1381. [CrossRef]
54. Hudon, C.; Lalonde, S.; Gagnon, P. Ranking the effects of site exposure, plant growth form, water depth, and transparency on aquatic plant biomass. *Can. J. Fish. Aquat. Sci.* **2000**, *57*, 31–42. [CrossRef]
55. Bornette, G.; Puijalon, S. Response of aquatic plants to abiotic factors: A review. *Aquat. Sci.* **2011**, *73*, 1–14. [CrossRef]
56. Middelboe, A.L.; Markager, S. Depth limits and minimum light requirements of freshwater macrophytes. *Freshw. Biol.* **1997**, *37*, 553–568. [CrossRef]
57. Fleming, J.P.; Madsen, J.D.; Dibble, E.D. Development of a GIS model to enhance macrophyte re-establishment projects. *Appl. Geogr.* **2012**, *32*, 629–635. [CrossRef]
58. Malczewski, J. On the Use of Weighted Linear Combination Method in GIS: Common and Best Practice Approaches. *Trans. GIS* **2000**, *4*, 5–22. [CrossRef]
59. Vanhellemont, Q. Adaptation of the dark spectrum fitting atmospheric correction for aquatic applications of the Landsat and Sentinel-2 archives. *Remote Sens. Environ.* **2019**, *225*, 175–192. [CrossRef]
60. Vanhellemont, Q.; Ruddick, K. Atmospheric correction of metre-scale optical satellite data for inland and coastal water applications. *Remote Sens. Environ.* **2018**, *216*, 586–597. [CrossRef]
61. Lee, Z.; Carder, K.L.; Arnone, R.A. Deriving inherent optical properties from water color: A multiband quasi-analytical algorithm for optically deep waters. *Appl. Opt.* **2002**, *41*, 5755. [CrossRef]
62. Lee, Z.; Weidemann, A.; Kindle, J.; Arnone, R.; Carder, K.L.; Davis, C. Euphotic zone depth: Its derivation and implication to ocean-color remote sensing. *J. Geophys. Res.* **2007**, *112*, C03009. [CrossRef]
63. Lee, Z. Penetration of solar radiation in the upper ocean: A numerical model for oceanic and coastal waters. *J. Geophys. Res.* **2005**, *110*, C09019. [CrossRef]

64. Havens, K.E. Submerged aquatic vegetation correlations with depth and light attenuating materials in a shallow subtropical lake. *Hydrobiologia* **2003**, *493*, 173–186. [CrossRef]
65. Abele, W. *Hydroacoustic Water Depth Dataset, Osterseen Lake District, Device*; Krupp Atlas Deso 10; Bavarian State Office for the Environment (LfU): Augsburg, Germany, 2001.
66. R Core Team. *R: A Language and Environment for Statistical Computing*; R Foundation for Statistical Computing: Vienna, Austria, 2022.
67. Pebesma, E.J. Multivariable geostatistics in S: The gstat package. *Comput. Geosci.* **2004**, *30*, 683–691. [CrossRef]
68. Graeler, B.; Pebesma, E.; Heuvelink, G. Spatio-Temporal Interpolation using gstat. *R J.* **2016**, *8*, 204–218. [CrossRef]
69. Florêncio, F.M.; Alves, D.C.; Lansac-Tôha, F.M.; Silveira, M.J.; Thomaz, S.M. The success of the invasive macrophyte *Hydrilla verticillata* and its interactions with the native *Egeria najas* in response to environmental factors and plant abundance in a subtropical reservoir. *Aquat. Bot.* **2021**, *175*, 103432. [CrossRef]
70. Azzella, M.M.; Bolpagni, R.; Oggioni, A. A preliminary evaluation of lake morphometric traits influence on the maximum growing depth of macrophytes. *J. Limnol.* **2014**, *73*, 400–406. [CrossRef]
71. Van Den Berg, M.S.; Scheffer, M.; Van Nes, E.; Coops, H. Dynamics and stability of Chara sp and Potamogeton pectinatus in a shallow lake changing in eutrophication level. *Hydrobiologia* **1999**, *408/409*, 335–342. [CrossRef]
72. Mõttus, M.; Sulev, M.; Baret, F.; Lopez-Lozano, R.; Reinart, A. Photosynthetically Active Radiation: Measurement and Modeling. In *Encyclopedia of Sustainability Science and Technology*; Meyers, R.A., Ed.; Springer: New York, NY, USA, 2012; pp. 7902–7932. [CrossRef]
73. Mobley, C. *The Oceanic Optics Book*; International Ocean Colour Coordinating Group (IOCCG): Dartmouth, NS, Canada, 2022.
74. Székely, G.J.; Rizzo, M.L.; Bakirov, N.K. Measuring and testing dependence by correlation of distances. *Ann. Stat.* **2007**, *35*, 2769–2794. [CrossRef]
75. Ramos-Carreño, C.; Torrecilla, J.L. dcor: Distance correlation and energy statistics in Python. *SoftwareX* **2023**, *22*, 101326. [CrossRef]
76. Lehmann, A. GIS modeling of submerged macrophyte distribution using Generalized Additive Models. *Plant Ecol.* **1998**, *139*, 113–124. [CrossRef]
77. Tang, R.W.K.; Doka, S.E.; Midwood, J.D.; Gardner Costa, J.M. Development and spatial application of a submerged aquatic vegetation model for Cootes Paradise Marsh, Ontario, Canada. *Aquat. Sci.* **2020**, *83*, 9. [CrossRef]
78. Harrow-Lyle, T.J.; Kirkwood, A.E. An ecological niche model based on a broad calcium-gradient reveals additional habitat preferences of the invasive charophyte Nitellopsis obtusa. *Aquat. Bot.* **2021**, *172*, 103397. [CrossRef]
79. Rey-Boissezon, A.; Auderset Joye, D. Habitat requirements of charophytes—Evidence of species discrimination through distribution analysis. *Aquat. Bot.* **2015**, *120*, 84–91. [CrossRef]
80. Miller, S.A.; Crowl, T.A. Effects of common carp (*Cyprinus carpio*) on macrophytes and invertebrate communities in a shallow lake. *Freshw. Biol.* **2006**, *51*, 85–94. [CrossRef]
81. Pípalová, I. Initial impact of low stocking density of grass carp on aquatic macrophytes. *Aquat. Bot.* **2002**, *73*, 9–18. [CrossRef]
82. Dörnhöfer, K.; Oppelt, N. Remote sensing for lake research and monitoring—Recent advances. *Ecol. Indic.* **2016**, *64*, 105–122. [CrossRef]
83. Calamita, E.; Lever, J.J.; Albergel, C.; Woolway, R.I.; Odermatt, D. Detecting climate-related shifts in lakes: A review of the use of satellite Earth Observation. *Limnol. Oceanogr.* **2024**, *39*, 723–741. [CrossRef]
84. Schaeffer, B.A.; Schaeffer, K.G.; Keith, D.; Lunetta, R.S.; Conmy, R.; Gould, R.W. Barriers to adopting satellite remote sensing for water quality management. *Int. J. Remote Sens.* **2013**, *34*, 7534–7544. [CrossRef]
85. Yates, K.L.; Bouchet, P.J.; Caley, M.J.; Mengersen, K.; Randin, C.F.; Parnell, S.; Fielding, A.H.; Bamford, A.J.; Ban, S.; Barbosa, A.M.; et al. Outstanding Challenges in the Transferability of Ecological Models. *Trends Ecol. Evol.* **2018**, *33*, 790–802. [CrossRef] [PubMed]
86. Hupfer, M.; Schwefel, R.; Jordan, S.; Köhler, A. *Auswirkungen des Klimawandels auf Seen in Deutschland*; Abschlussbericht; Länderarbeitsgemeinschaft Wasser (LAWA-AK): Berlin, Germany, 2022.
87. Hoffmann, M.; Raeder, U. Predicting the potential distribution of neophytes in Southern Germany using native Najas marina as invasion risk indicator. *Environ. Earth Sci.* **2016**, *75*, 1217. [CrossRef]